Extraordinary Coherent Thermal Emission From SiC Due to Coupled Resonant Cavities

Nir Dahan
Avi Niv
Gabriel Biener
Yuri Gorodetski
Vladimir Kleiner
Erez Hasman
e-mail: mehasman@tx.technion.ac.il

Faculty of Mechanical Engineering,
Micro and Nanooptics Laboratory,
Russell Berrie Nanotechnology Institute,
Technion-Israel Institute of Technology,
Haifa 32000, Israel

In high temperature and vacuum applications, when heat transfer is predominantly by radiation, the material's surface texture is of substantial importance. Several micro- and nanostructure designs have been proposed to enhance a material's emissivity and its radiative coherence, as control of thermal emission is of crucial concern in the design of infrared sources, optical filters, and sensing devices. In this research, an extraordinary coherent thermal emission from an anisotropic microstructure is experimentally and theoretically presented. The enhanced coherency is due to coherent coupling between resonant cavities obtained by surface standing waves, wherein each cavity supports a localized field that is attributed to coupled surface phonon polaritons. We show that it is possible to obtain a polarized quasimonochromatic thermal source from a SiC microstructure with a high quality factor of 600 at the resonant frequency of the cavity and a spatial coherence length of 716 wavelengths, which corresponds to an angular divergence of 1.4 mrad. In the experimental results, we measured a quality factor of 200 and a spatial coherence length of 143 wavelengths. We attribute the deviation in the experimental results to imperfections in the fabrication of the high quality factor cavities.
[DOI: 10.1115/1.2955475]

Keywords: coherence, thermal emission, resonators, surface waves

1 Introduction

The thermal emission of absorbing materials is affected by surface morphology as well as the excitation of surface waves, surface plasmon polaritons in metal, or surface phonon polaritons (SPPs) in polar crystal [1–3]. Surface waves are confined electromagnetic waves due to collective oscillations of the free electrons in metal or the resonant collective lattice vibrations in polar crystal, which propagate along the interface and decay exponentially with increasing the distance from the interface [4,5]. The electromagnetic energy density associated with surface waves has been widely investigated. It has been shown that thermal emission can be quasimonochromatic in the vicinity of a flat surface, in a distance that is of the order of a wavelength, due to the excitation of resonant surface waves [6]. Furthermore, surface modes yield a long-range spatial coherence length, L_c, on a scale of the surface wave propagation length, $L_{\|}$, which may be much larger than the emitted wavelength, $L_c \approx L_{\|} \gg \lambda$ [7,8]. To transmit these surface waves along with their coherency to the far field, several configurations were suggested to design thermal sources, such as gratings [9,10], multilayer structure [11,12], photonic crystals [13–15], and resonant cavities [16,17]. In the far field, the spatial coherence can be evaluated by the directivity of the emitted wave via $l_c \sim \lambda/(\Delta\theta \cos\theta)$, where $\Delta\theta$ is the angular lobe. In the case of introducing a shallow grating coupler ($h \ll \lambda$), a smooth perturbation is caused to the surface [1]; therefore, the emission pattern had a rainbowlike behavior, and the coherence length in the far field, l_c, was found to be limited by that of the delocalized surface waves ($l_c \leq L_c$) [7,9].

An alternative way of analyzing thermal emission, according to Kirchhoff's law, is by determining the absorptivity of a structure. Using a relatively deep grating ($h \sim \lambda$), strong radiation absorption was obtained over a broad range of incident angles due to localized field enhancement. This absorption was attributed to the excitation of standing wave coupled surface plasmons in narrow grating cavities [18].

In this paper, we investigate theoretically and experimentally an extraordinary coherent thermal radiation of coupled resonant cavity (CRC) structure that was etched on a silicon carbide (SiC-6*H* polytype) substrate. Herein, the implementation of CRC is extended to crystalline material where the delocalized SPPs have a long-range coherency in the near field ($L_c = 55\lambda$), consecutive to our recent work on amorphous fused silica, where the spatial coherence of the radiative field was enhanced by an order of magnitude compared to the small delocalized SPP coherency ($l_c = 32\lambda \gg L_c = 2\lambda$) [17]. Here, we show that it is possible to obtain a quasimonochromatic thermal source with a high quality factor $Q = \omega/\Delta\omega \approx 600$, which corresponds to highly temporal coherence and a spatial coherence length of the radiative field $l_c \approx 716\lambda$. This coherence length is enhanced compared with the coherency of the delocalized SPPs and therefore is encouraged to design highly coherent and unidirectional infrared (IR) sources, e.g., for spectroscopy or selective detectors. Moreover, our source has a peculiar behavior: It supports a thermal emission at a single resonant frequency and in a well-defined direction. Note that this emission distribution is fundamentally different than coupling delocalized SPPs using a prism or grating coupler whereby each frequency is emitted in a different direction according to the dispersion relation of the delocalized SPPs. This resonant enhancement could be obtained for a TM polarized wave (as illustrated in Fig. 1(*a*)) due to CRC structure in the spectral range where SiC supports SPPs. The CRC structure consists of periodic cavities in which each cavity supports standing waves and adjacent cavities are coupled by surface standing waves.

2 Theoretical Analysis and Experimental Results

The coherent thermal emission can be viewed as the interplay between two mechanisms. The first is a localized field inside the cavity. A single resonant frequency is supported by the cavity according to its geometry, i.e., width, depth, shape, and the nature

Contributed by the Heat Transfer Division of ASME for publication in the JOURNAL OF HEAT TRANSFER. Manuscript received October 10, 2007; final manuscript received March 26, 2008; published online September 3, 2008. Review conducted by Jayathi Murthy.

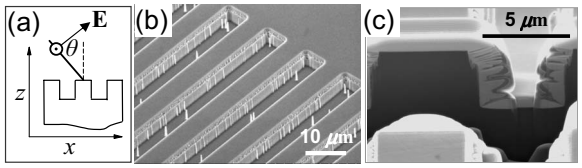

Fig. 1 (*a*) CRCs geometry with a coordinate system. (*b*) SEM image of CRC structure. (*c*) SEM image of a single cavity cross section embedded in SiC with periodicity $\Lambda=11.6$ μm, fill factor $q=0.56$, and depth $h=4.6$ μm; to observe the cavity profile in a high contrast (the dark region indicates SiC), a Pt was deposited and ion milling with a focused ion beam was performed.

of the substrate material. The magnitude of the TM polarized electric field was calculated by a finite difference time domain (FDTD) algorithm, as shown in Fig. 2(*a*) for deep resonant cavities. Standing waves are clearly discerned inside the cavities, which originate from coupled SPPs that decay from the inner cavity walls; this results in a greater energy density being observed along the walls. Each isolated cavity can be regarded as a localized source supporting a broad angular emission. In order to obtain a directional emission, a coherent coupling mechanism between the cavities is required. Otherwise, the emission behavior would be according to the localized field, which is omnidirectional [19]. By choosing the periodicity of the cavities according to Rayleigh's anomaly, a surface standing wave is excited by the first diffraction order, as shown in Fig. 2(*b*), which correlates adjacent resonant cavities. As a result, we obtained a resonant frequency having a coherency for a longer distance than that of the delocalized SPPs, yielding a highly directional emission.

We studied the thermal emission by realizing a CRC structure embedded in SiC substrate. SiC is an interesting candidate as a thermal source since it has a high melting temperature, a low thermal expansion, and specialized by a high mechanical strength. As a polar crystal, SiC supports SPPs in the spectral range where $\tilde{\varepsilon}'<-1$, corresponding to the IR spectra between 10.6 μm and 12.6 μm, having a complex dielectric constant of $\tilde{\varepsilon}(\lambda_0=11.6\ \mu\text{m})=\tilde{\varepsilon}'+i\tilde{\varepsilon}''=-11.9+i0.62$ [20]. Our structure was designed to support directional thermal emission at $\lambda_0=11.6$ μm wavelength in the normal direction. For this purpose, the periodicity was set to be equal to the wavelength $\Lambda=\lambda_0$. Because of the high Q, the resonant frequency is sensitive to the cavity shape; therefore, the final depth h was fine-tuned accordingly to be $h=4.6$ μm with a filling factor $q=0.56$. We fabricated a 15 mm square CRC structure by standard photolithographic technique using a negative photoresist. After developing the photoresist, a NiCr of thickness 1300 Å was deposited and afterward lift-off was performed. The substrate was etched through the NiCr mask by reactive ion etching at a power of 250 W and a pressure of

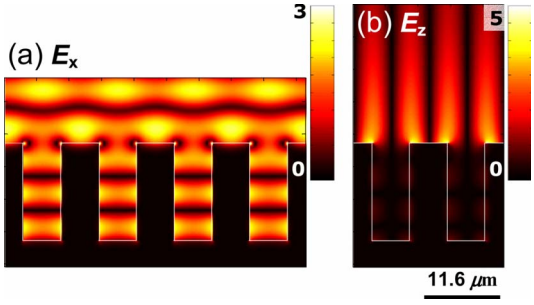

Fig. 2 The magnitude of the electric field components in the *x-z* plane, (*a*) $|E_x|$ and (*b*) $|E_z|$, for normal incident wavelength $\lambda_0=11.6$ μm. The calculations were performed for a SiC CRC with periodicity $\Lambda=11.6$ μm, fill factor $q=0.5$, and depth $h=14.85$ μm.

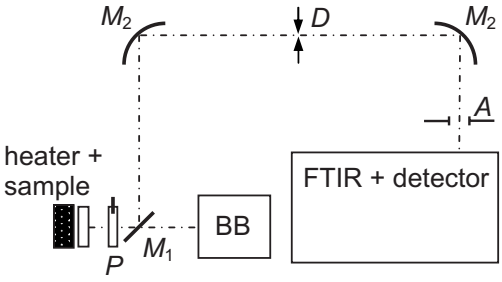

Fig. 3 Experimental setup used to measure spectral directional emissivity. *P*-polarizer; BB-blackbody; M_1-flat mirror on rotating stage; M_2-parabolic mirror, focal length=250 mm; *D*-angular resolution diaphragm in the focal plane of M_2, diameter=1 mm; *A*-field of view aperture; diameter=10 mm.

10 mTorr with SF_6 and O_2 gases at flow rates of 19 SCCM and 1 SCCM, respectively (SCCM denotes cubic centimeter per minute at STP). The etching was performed at a rate of 600 Å/min at room temperature until the desired depth was reached. As a final step, the remaining NiCr was removed with a Cr etchant. Scanning electron microscope (SEM) images of the structure and the cavity cross section are shown in Figs. 1(*b*) and 1(*c*), respectively. Submicron rods remained after the etching process inside the cavities, as shown in Fig. 1(*b*). They are located randomly inside the cavities and upon the sample with a typical diameter of 400 nm, which is much smaller than the emitted wavelength. Thus, we neglect them in our calculations.

The experimental setup that was used to measure the spectral directional emissivity is illustrated in Fig. 3. The sample and the blackbody (CI-Systems, Model SR-80-4HT) were heated to $T=770\pm1$ K to increase the radiative flux and improve the signal-to-noise ratio. The sample temperature was measured with a K-type thermocouple and controlled by a temperature controller (HeatWave Labs, Model 101303-04B). Measurements of the emission spectra were performed using a Fourier transform IR spectrometer (FTIR, Bruker-Vertex 70) equipped with a cooled HgCdTe detector. The spectral resolution was set to $\delta\omega=1$ cm^{-1}, the field of view $A=10$ mm, and an angular resolution $\Omega=2.4\times10^{-6}$ sr (corresponding to $\delta\theta=0.1$ deg). Note that the measured emissivity ($\bar{\varepsilon}$) is actually an averaged emissivity over the solid angle Ω, i.e., $\bar{\varepsilon}(\omega\pm\delta\omega/2,\theta\pm\delta\theta/2,T)=\int_\Omega\varepsilon(\omega\pm\delta\omega/2,\theta,T)d\Omega'$. The calculated emissivity was derived from the calculations of the reflectivity using rigorous coupled wave analysis (RCWA). Figure 4(*a*) shows the emissivity distribution in the (θ,ω) plane calculated for a rectangular cavity configuration shown in Fig. 1(*a*). The measured emissivity (normalized to a blackbody) is given in Fig. 4(*b*). Both figures are for TM polarization state at the spectral range that supports SPPs. A bright spot is observed in the center, which indicates high emission. This thermal source is quasimonochromatic—it supports only a very narrow spectral band—and is highly directional. Although a signature pattern of frequencies emitted in off-axis directions is observed in Fig. 4, the image confirms a low emissivity, resulting from less effective support by the cavity. The measured and the calculated spectral emissivity near the normal direction at $\theta=0$ deg and $\theta=1$ deg are shown in Fig. 5(*a*) for the realized cavity profile, as depicted in the inset of Fig. 5(*a*). A narrow spectral peak, $\Delta\omega=1.41$ cm^{-1} (corresponding to $\Delta\lambda=20$ nm) at half maximum, is theoretically observed around $\omega_0=862$ cm^{-1} (11.6 μm) having a quality factor $Q=\omega_0/\Delta\omega\approx600$. Figure 5(*b*) shows measured and calculated angular emissivities at the peak frequencies observed in Fig. 5(*a*). As can be seen, there is a single resonance peak at the frequency that is supported by the cavity and satisfies the standing wave between the cavities (black). At nearby frequency (red), the emissivity drops and the angular lobes are much broader, which corresponds to smaller spatial coherency. The calculated lobe width at half

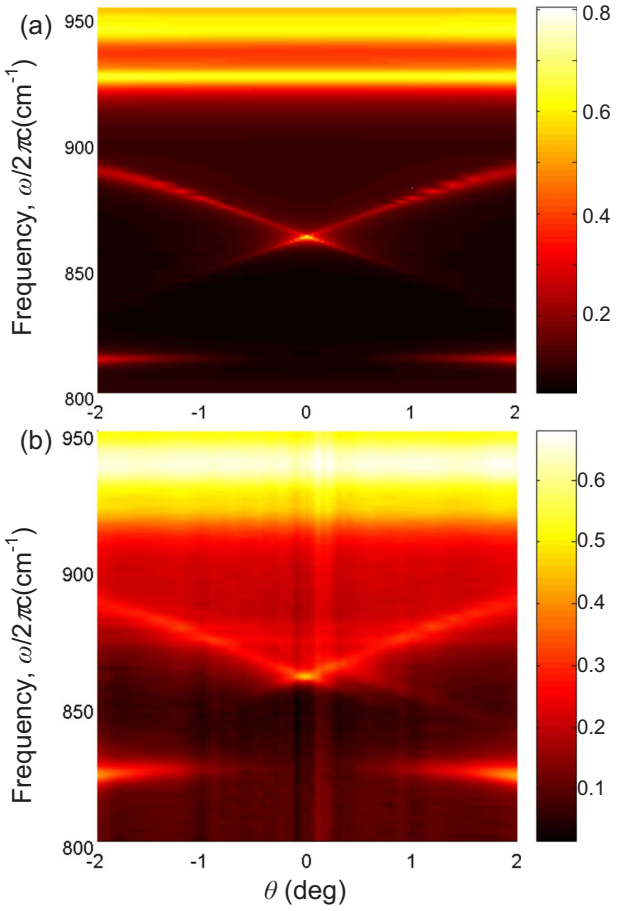

Fig. 4 (***a***) **Calculated emissivity, ε, for rectangular cavity profile shown in Fig. 1(*a*) and (*b*) measured emissivity, $\bar{\varepsilon}$, distribution as a function of frequency in the spectral range in which SiC supports SPPs, and the observation angle near the normal direction. The bright colors represent high emissivity.**

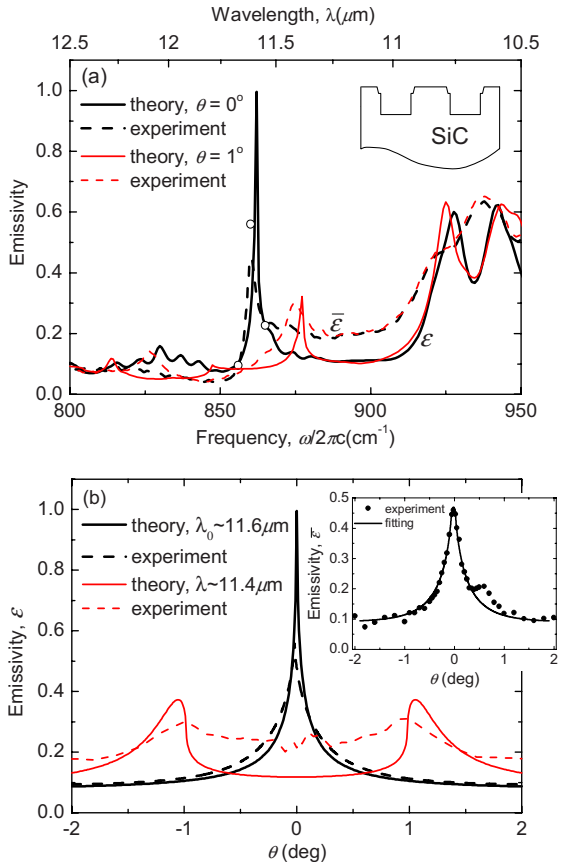

Fig. 5 (***a***) **Spectral emissivity observed in (thick line) a normal direction and in (thin line) θ=1 deg for TM polarized wave; (solid) calculated emissivity for the realized cavity profile as illustrated in the inset, (dash) experiment, and (circle) corrected emissivity obtained from (*b*). (*b*) Angular emissivity at the peak wavelengths obtained in (*a*); (solid) theory and (dash) experiment obtained by deconvolution analysis. The inset shows (dots) the measured emissivity and the (solid) curve fitting to the experimental results obtained by convolving the dash curve in (*b*) and the angular resolution.**

maximum, $\Delta\theta$=0.08 deg=1.4 mrad, is a signature to the spatial coherence length of the thermal radiation. The relation between the angular deviation of the beam and the spatial coherence length is known as $l_c \approx \lambda/\Delta\theta$, herein, $l_c \approx 716\lambda_0 \approx 8.3$ mm; slightly smaller than Aperture *A*. Note that this spatial coherence length is significantly higher than the propagation length of SPPs on a flat SiC-vacuum interface, which equals approximately the coherence length of the delocalized surface waves, $L_{\|} \approx 1/\mathrm{Im}(k_{\|}) \approx 55$ μm, where $k_{\|}=(\omega/c)\sqrt{\tilde{\varepsilon}(\omega)/(\tilde{\varepsilon}(\omega)+1)}$ is the SPPs' wave number [7]. The experimental results depicted in Fig. 5(*a*) and 5(*b*) show a reasonable agreement with the calculation. Herein, the theoretical lobe width is of the order of the angular resolution we have used in our experiment ($\Delta\theta \sim \delta\theta$). As a result, the measured emissivity $(\bar{\varepsilon}(\omega \pm \delta\omega/2, \theta \pm \delta\theta/2, T))$ is smaller than the real emissivity $(\varepsilon(\omega \pm \delta\omega/2, \theta, T))$ at the resonance frequency near the normal direction (see inset in Fig. 5(*b*)). In order to retrieve the emissivity distribution we have used deconvolution analysis. The emissivity peak shown in Fig. 5(*b*) equals 0.56 with an angular width at half maximum $\Delta\theta$=0.4 deg, which corresponds to a spatial coherence $L_c \approx 143\lambda_0$. Using this result, we corrected the spectral emissivity at the peak frequency in Fig. 5(*a*) to be 0.56 as well (circle), with an estimated quality factor $Q \sim 200$. We attribute the deviation in the coherency values to the high sensitivity of the structure in the cavity geometry, roughness, and defects due to the behavior of the high Q cavity.

In order to understand the physical origin of the enhanced coherency, we calculated the reflectivity as a function of the cavity depth for the actual cavity profile shown in Fig. 1(*c*). Figure 6 shows the reflectivity for TM polarized light at 11.6 μm wavelength using RCWA. The sharp dips resemble a Fabry–Pérot-like resonator, which indicates its high Q. The difference between two successive depths $h_{m+1}-h_m$ is equal to half of the wavelength of the standing wave inside the cavity, λ^{sw} [18]. In our case, for incident vacuum wavelength of 11.6 μm, we obtained $\lambda^{sw}=10.4$ μm with the corresponding wave number $k^{sw}=2\pi/\lambda^{sw}$.

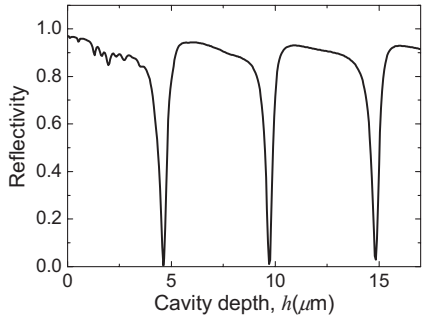

Fig. 6 Calculated reflectivity of CRC as a function of the cavity depth, for normal incident wavelength λ_0=11.6 μm

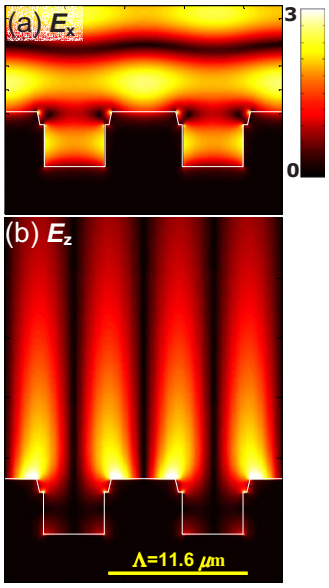

Fig. 7 The magnitude of the electric field components in the *x-z* plane, (*a*) $|E_x|$ and (*b*) $|E_z|$, for normal incident wavelength λ_0=11.6 μm. The calculations were performed for the realized cavity profile as shown in Fig. 1(*c*): periodicity Λ=11.6 μm, fill factor q=0.56, and depth h=4.6 μm.

The depth of the realized cavity was determined to be the first dip due to fabrication considerations. Figure 7 shows the calculated field distribution using FDTD algorithm for the realized structure having the cavity parameters, as shown in Fig. 1(*c*). Figure 7(*a*) shows the electric field localized inside the cavity whereas Fig. 7(*b*) shows the horizontal standing wave between adjacent cavities. We confirmed that the observed standing waves inside the cavity are due to the coupled SPPs from the vertical walls inside the cavity by solving the characteristic equation of an infinite slab waveguide [21], an air gap between two semi-infinite layers of lossy material, herein SiC. The wave number of the coupled surface wave is calculated as

$$\beta = \left\{ k_0^2 + \frac{2}{\tilde{\varepsilon}^2 d^2}\left[1 + \sqrt{1 + k_0^2 \tilde{\varepsilon}^2 d^2 (1+\tilde{\varepsilon})}\right] \right\}^{1/2} \quad (1)$$

where $k_0 = 2\pi/\lambda_0$ is the wave number of the incident wave in a vacuum and d is the width of the slab, which equals the cavity width $d = \Lambda(1-q) \approx 5.1$ μm. Equation (1) is valid under the approximation that $d \ll 2\delta_{air}$, where δ_{air} is the decay length of the SPPs in air, which is evaluated by $\delta_{air} = 1/|\mathrm{Im}\sqrt{k_0^2 - k_\parallel^2}| \approx 5.7$ μm. The dispersion relation of the waveguide mode wave number, β, given by Eq. (1) is shown in Fig. 8(*a*) along with k^{sw} and the

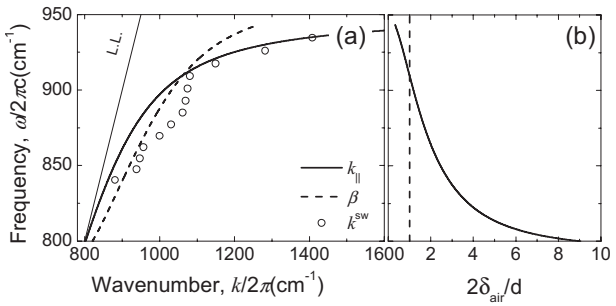

Fig. 8 (*a*) Dispersion relation of SPPs at SiC flat surface $k_\parallel$, i.e., delocalized (solid); slab waveguide β (dashed); standing waves inside the cavity k^{sw} (dots). (*b*) Decay length of delocalized SPPs in air as a function of frequency.

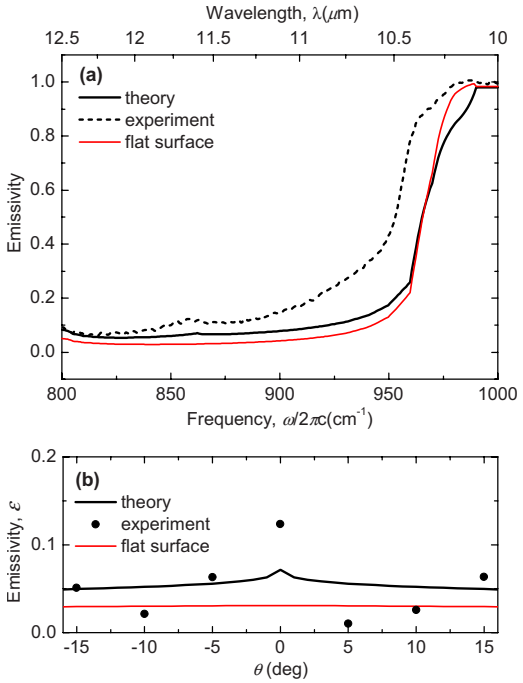

Fig. 9 (*a*) Spectral emissivity observed in normal direction for TE polarized wave and (*b*) angular emissivity at the peak wavelength at 11.6 μm, obtained in (*a*).

delocalized SPPs $k_\parallel$. Two regimes are discerned: above and beneath the intersection of $k_\parallel$ and β. Beneath the intersection point, k^{sw} behaves like β, whereas above it behaves like $k_\parallel$. It can be understood according to the decay length of SPP in air as shown in Fig. 8(*b*), where the intersection point corresponds to a decay length of half the cavity width. Our calculations showed an enhanced coherent emission at frequencies below the intersection point, while above it the coherency was similar to that of the delocalized SPPs. Thus, coupled SPPs inside the cavity are necessary to obtain enhanced coherency. A horizontal standing wave at the same frequency is excited on the rib between the cavities (see Fig. 7(*b*)), designated to link adjacent cavities for a long distance on the interface; evidence of the high directivity of the spontaneous emission. The CRC structure can also be understood as a coherent coupled antenna array; each cavity can be regarded as an IR antenna consisting of a wire with a length of a half-wavelength ($\lambda^{sw}/2$) at the operating frequency [22].

Finally, the thermal emission from CRC structure was characterized for TE polarization state. SPPs do not exist in SiC at TE polarized light; hence, no emission enhancement is expected. We measured and calculated the spectral emissivity in the normal direction (Fig. 9(*a*)) and the directional emissivity at 11.6 μm (Fig. 9(*b*)). A low omnidirectional emissivity was observed close to that of a flat surface. The small enhancement is obtained due to a guided mode mechanism, which is affected by the cavity dimension (geometric resonance). The geometric resonance appears as long as the cavity width is larger than the cutoff width $d_c \sim (\lambda/\pi)\tan^{-1}\sqrt{-\tilde{\varepsilon}'}$, for a lossy infinite waveguide [23]. In our structure d_c=4.76 μm, slightly smaller than the cavity width, which confirms the existence of geometric resonance. These resonances become the dominant mechanism for enhanced emission in very deep cavities. For example, the emissivity for a TE wave can reach 0.8 at ~100 μm cavity depth.

3 Conclusions

In conclusion, by utilizing periodic CRCs, a very highly coherent and polarized thermal source can be designed, e.g., for IR

spectrometers, that is not limited by the coherence of the delocalized SPPs. This enhancement is obtained due to the increasing photonic density of states inside the cavity by localized surface waves, coupling adjacent cavities by horizontal standing wave, and coherent coupling into radiative. The high resonance structure might be utilized also in absorption mechanism for multispectral thermal detectors as well as for IR sensing devices.

Nomenclature

c = speed of light in vacuum
d = cavity width
d_c = cutoff width
h = cavity height
k = wave number
$k_{\|}$ = SPPs wave number
l_c = spatial coherence length in the far field
$L_{\|}$ = surface wave propagation length
L_c = spatial coherence length in the near field
q = filling factor
Q = quality factor
β = waveguide wave number
δ = decay length, $\delta = 1/\mathrm{Im}(k_z)$
ε = theoretical spectral directional emissivity
$\bar{\varepsilon}$ = experimental spectral directional emissivity
$\tilde{\varepsilon}$ = dielectric constant, relative electric permittivity
λ = wavelength
λ^{sw} = wavelength of a standing wave
Λ = periodicity of CRC structure
θ = polar emission angle
ω = angular frequency
Ω = solid angle

References

[1] Greffet, J.-J., Carminati, R., Joulain, K., Mulet, J.-P., Mainguy, S., and Chen, Y., 2002, "Coherent Emission of Light by Thermal Sources," Nature (London), **416**, pp. 61–63.
[2] Fu, C. J., Zhang, Z. M., and Tanner, D. B., 2005, "Planar Heterogeneous Structures for Coherent Emission of Radiation," Opt. Lett., **30**, pp. 1873–1875.
[3] Sai, H., Yugami, H., Akiyama, Y., Kanamori, Y., and Hane, K., 2001, "Spectral Control of Thermal Emission by Periodic Microstructured Surfaces in the Near-Infrared Region," J. Opt. Soc. Am. A, **18**, pp. 1471–1476.
[4] Boardman, A. D., 1982, *Electromagnetic Surface Modes*, Wiley, Belfast, Ireland.
[5] Raether, H., 1988, *Surface Plasmons*, Springer-Verlag, Berlin.
[6] Shchegrov, A. V., Joulain, K., Carminati, R., and Greffet, J.-J., 2000, "Near-Field Spectral Effects Due to Electromagnetic Surface Excitations," Phys. Rev. Lett., **85**, pp. 1548–1551.
[7] Carminati, R., and Greffet, J.-J., 1999, "Near-Field Effects in Spatial Coherence of Thermal Sources," Phys. Rev. Lett., **82**, pp. 1660–1663.
[8] Setälä, T., Kaivola, M., and Friberg, A. T., 2002, "Degree of Polarization in Near Fields of Thermal Sources: Effects of Surface Waves," Phys. Rev. Lett., **88**, p. 123902.
[9] Laroche, M., Arnold, C., Marquier, F., Carminati, R., Greffet, J.-J., Collin, S., Bardou, N., and Pelouard, J.-L., 2005, "Highly Directional Radiation Generated by a Tungsten Thermal Source," Opt. Lett., **30**, pp. 2623–2625.
[10] Hesketh, P. J., Zemel, J. N., and Gebhart, B., 1988, "Polarized Spectral Emittance From Periodic Micromachined Surfaces. I. Doped Silicon: The Normal Direction," Phys. Rev. B, **37**, pp. 10795–10802.
[11] Lee, B. J., and Zhang, Z. M., 2007, "Coherent Thermal Emission From Modified Periodic Multilayer Structures," ASME J. Heat Transfer, **129**, pp. 17–26.
[12] Ben-Abdallah, P., 2004, "Thermal Antenna Behavior for Thin-Film Structures," J. Opt. Soc. Am. A, **21**, pp. 1368–1371.
[13] Yablonovitch, E., 1987, "Inhibited Spontaneous Emission in Solid-State Physics and Electronics," Phys. Rev. Lett., **58**, pp. 2059–2062.
[14] Chan, D. L. C., Soljačić, M., and Joannopolous, J. D., 2006, "Thermal Emission and Design in 2D-Periodic Metallic Photonic Crystal Slabs," Opt. Express, **14**, pp. 8785–8796.
[15] El-Kady, I., Chow, W. W., and Fleming, J. G., 2005, "Emission From an Active Photonic Crystal," Phys. Rev. B, **72**, p. 195110.
[16] Celanovic, I., Perreault, D., and Kassakian, J., 2005, "Resonant-Cavity Enhanced Thermal Emission," Phys. Rev. B, **72**, p. 075127.
[17] Dahan, N., Niv, A., Biener, G., Gorodetski, Y., Kleiner, V., and Hasman, E., 2007, "Enhanced Coherency of Thermal Emission: Beyond the Limitation Imposed by Delocalized Surface Waves," Phys. Rev. B, **76**, p. 045427.
[18] Sobnack, M. B., Tan, W. C., Wanstall, N. P., Preist, T. W., and Sambles, J. R., 1998, "Stationary Surface Plasmons on a Zero-Order Metal Grating," Phys. Rev. Lett., **80**, pp. 5667–5670.
[19] Dahan, N., Niv, A., Biener, G., Kleiner, V., and Hasman, E., 2005, "Space-Variant Polarization Manipulation of a Thermal Emission by a SiO_2 Subwavelength Grating Supporting Surface Phonon-Polaritons," Appl. Phys. Lett., **86**, p. 191102.
[20] Palik, E. D., 1985, *Handbook of Optical Constants of Solids*, Academic, Orlando, FL.
[21] Yang, F., Sambles, J. R., and Bradberry, G. W., 1991, "Long-Range Surface Modes Supported by Thin Films," Phys. Rev. B, **44**, pp. 5855–5872.
[22] Mühlschlegel, P., Eisler, H.-J., Martin, O. J. F., Hecht, B., and Pohl, D. W., 2005, "Resonant Optical Antennas," Science, **308**, pp. 1607–1609.
[23] Gordon, R., and Brolo, A. G., 2005, "Increased Cut-Off Wavelength for a Subwavelength Hole in a Real Metal," Opt. Express, **13**, pp. 1933–1938.